Workshop on Monte Carlo Tools for the LHC

CERN, July 8th 2003

Parton String Model

N. Armesto

Theory Division
CERN

N.S.Amelin, NA, C.Pajares and D.Sousa, Eur.Phys.J.C22(2001)149;
NA, C.Pajares and D.Sousa, Phys.Lett.B527(2002)92.

Contents:

1. Introduction

Absolutely ambitious: from $\tau = 0$ to decays

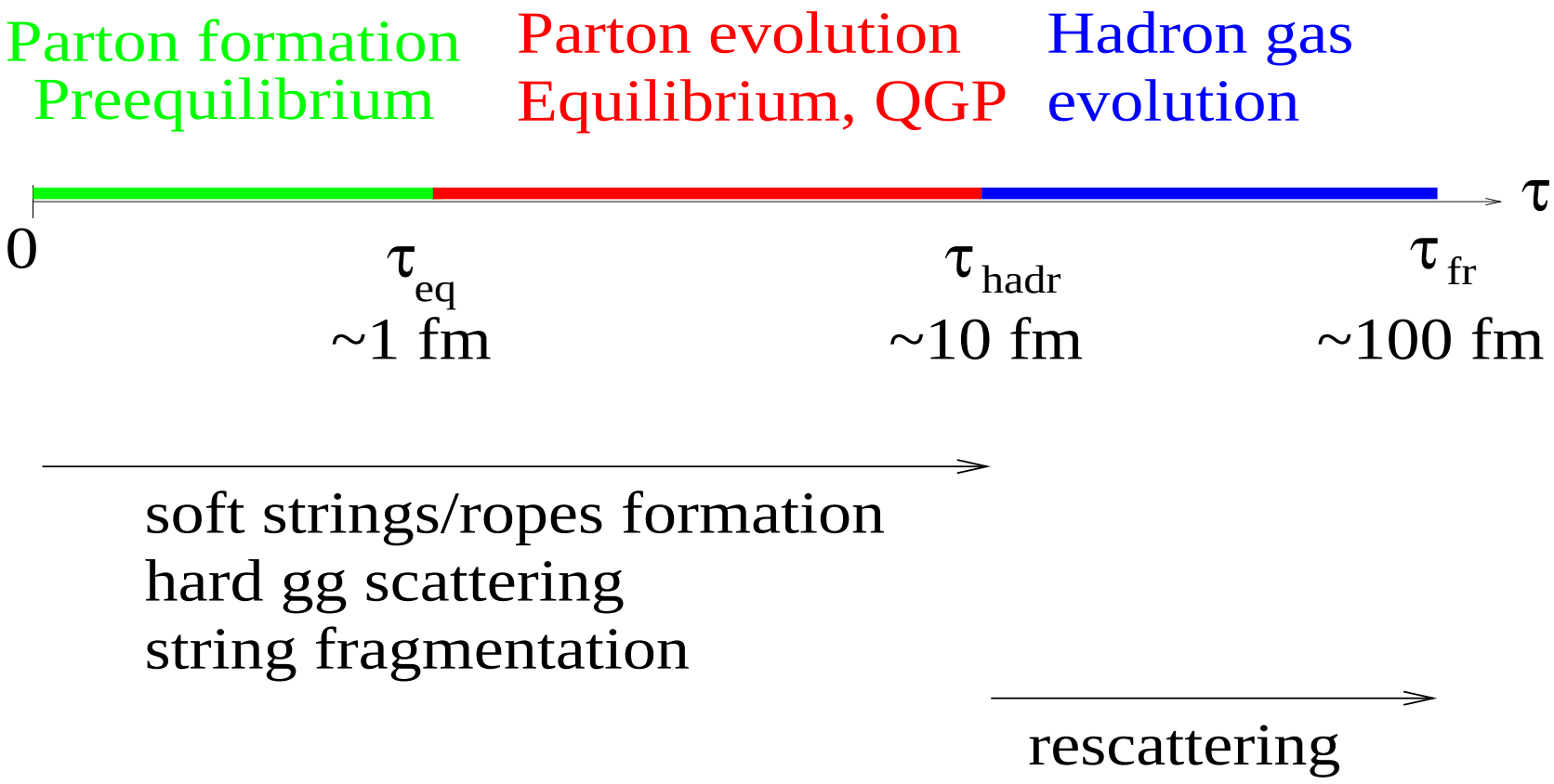

2. Physical content:

2.1 Nucleon and parton sampling

• Impact parameter is generated on geometrical basis (uniform distribution with measure d^2b).

• Nucleon positions in transverse space are sampled according to a Woods-Saxon for A $>$ 11,

$$\rho(r) = \frac{\rho_0}{1+\exp[(r-r_n)/a]} \ ,$$
$$r_n = 1.07 \ \mathrm{A}^{1/3} \ \ \mathrm{fm}, \quad a = 0.545 \ \ \mathrm{fm}, \tag{1}$$

and Gaussian for A $\leq$ 11, with parameters chosen for each nucleus.

• Fermi motion is given to the nucleons, uniformly in the range $0 < p < p_F$, with

$$p_F = h\ [3\pi\rho(r)]^{1/3}, \quad h = 0.197 \ \text{ fm GeV/c}. \tag{2}$$

• Partons are generated for each nucleon. Its number is given by a quasieikonal (V.A.Abramovsky et al., SJNP 53 (91) 271)

$$\begin{aligned} W_N &= C_N\ e^{-g(s)C/2}\ \frac{[Cg(s)/2]^N}{CN!/2}\ , \\ g(s) &= g_0 s^{\Delta/2}, \quad g_0 = \frac{8\pi\gamma_P}{\sigma_P}, \end{aligned} \tag{3}$$

with $\Delta = 0.139$, $C = 3.0$, $\gamma_P = 1.77$ GeV^2 and $\sigma_P = 3.3$ mb.

• Parton flavors are valence quarks and diquarks, and sea pairs with $u : d : s = 1 : 1 : 0.26$.

• Parton positions in transverse space (inside a nucleon) are given by a Gaussian,

$$F(b) = \frac{1}{4\pi\lambda}\ \exp\left(-\frac{b^2}{4\lambda}\right), \quad \lambda = R_0^2 + \alpha' \ln s, \tag{4}$$

with $R_0^2 = 3.18$ GeV^2 and $\alpha' = 0.21$ GeV^2.

2.2 String formation

• One parton from the projectile and one from the target produce an inelastic collision if both lie within an area in impact parameter equal to $\sigma_P = 2\pi r_P^2$, $r_P = 0.23$ fm.

• Cross sections are computed in the quasieikonal model (A.B.Kaidalov, SJNP 45 (87) 902; Yu.M.Shabelsky, ZPC57 (93) 409),

$$\sigma_{tot} \quad = \quad \sigma_P\ f(z/2),$$

$$
\begin{aligned}
z &= \frac{C\gamma_P s^{\Delta}}{\lambda} \ , \quad f(z) = \sum_{k=1}^{\infty} \frac{(-z)^{k-1}}{k \cdot k!} \ , \\
\sigma_{el} &= \frac{2\sigma_P}{C} \left[f(z/2) - f(z) \right], \\
\sigma_{diff} &= \left(C/2 - 1 \right) \sigma_{el} \ , \qquad (5)
\end{aligned}
$$

which reduces to the eikonal for $C = 2$.

- An inelastic collision is hard (two-component model) with probability

$$
W_h = \frac{C_h \ (s - s_0)^{\Delta_h}}{C_h \ (s - s_0)^{\Delta_h} + s^{\Delta}} \ , \qquad (6)
$$

with $\Delta_h = 0.50$, $\sqrt{s_0} = 25$ GeV and $C_h = 0.0035$. It will proceed, in the standard way, through PYTHIA 5.5 + ARIADNE 4.02 + JETSET 7.3, with $p_{\perp min} = 3.03 + 0.11 \ln (s/s_0)$ GeV/c.

• From the total cross section in (5), the elastic, hard, and production cross sections are computed.

• Diffraction is not properly taken into account in the model; besides, a Reggeon contribution is needed at SPS energies.

• Soft collisions give two strings, as in DPM/QGSM (ABK, ibid.; A.Capella et al., PR236 (94) 225).

• Hard collisions are $gg \longrightarrow gg$.

• For the string ends coming from one nucleon of the projectile or target, longitudinal momentum fractions are distributed as

$$\begin{aligned} L(x_1, x_2, \ldots, x_n) &= f_{qq}(x_1) f_q(x_2) \ldots f_q(x_n), \\ \sum_{k=1}^{n} x_k &= 1. \end{aligned} \tag{7}$$

• For soft strings (QGSM),

$$f_{qq}(x) = x^{3/2}, \quad f_q(x) = \frac{1}{\sqrt{x}} \ , \tag{8}$$

with a lower cut-off $x_{min} = 0.3 \text{ GeV}/\sqrt{s_{NN}}$.

• For hard collisions, PDFLIB parton densities + nuclear corrections are used (default: GRV 94 LO + EKS98, but little sensitivity to this choice).

• Transverse momentum of a string end coming from a nucleon which has been wounded m times is given (AC et al., EPJC11 (99) 163), according to (4), by a Gaussian,

$$T(p_\perp) = \frac{1}{\pi\delta^2} \, e^{-p_\perp^2/\delta^2}, \quad \delta = 0.5 \, \sqrt{m} \ \text{ GeV/c}. \tag{9}$$

• Two soft inelastic collisions fuse (i.e. two strings are created instead of four) when their transverse positions are within an area σ_f. This becomes more important with increasing string density (central AB collisions and high energies).

• Just (effective) fusion of two strings is considered:

$$\sigma_f = 2\pi r_f = 7.5 \ \ \mathrm{mb} > \sigma_P = 3.3 \ \ \mathrm{mb}, \tag{10}$$

which gives $r_f = 0.35$ fm.

• Energy-momenta of the fusing string ends sum into the energy-momentum of the fused string ends.

• The new strings belong to representations of SU(3):

$$3 \otimes 3 = 6 \oplus \overline{3}, \quad 3 \otimes \overline{3} = 1 \oplus 8, \tag{11}$$

and the fused string tension follows Casimir scaling (G.Bali, PRD62 (00) 114503; PR343 (01) 1; Yu.A.Simonov, JETPL71 (00) 127; YuAS et al., PRL85 (00) 1811).

• Only fusion of two soft strings is considered (transverse size of a string $\propto 1/\langle p_\perp \rangle$); some effect is to be expected at LHC (32 % hard collisions in central PbPb).

2.3 Hadronization

• For strings coming from hard partons, JETSET is used

• For soft strings, masses are generated according to Schwinger model:

$$W \propto K_{\{N\}}^2 \exp\left(-\pi M^2/K_{\{N\}}\right), \tag{12}$$

longitudinal momentum breaking follows the Artru-Mennessier area law:

$$P \propto \exp\left(-bA\right), \quad K_{\{N\}} \propto bC_{\{N\}}^2, \quad A = p_+ p_- \tag{13}$$

and transverse momentum is sampled according to a Gaussian:

$$f(p_T^2) \propto \exp\left(-\alpha_{\{N\}} p_T^2\right), \tag{14}$$

with $K_{\{3\}} = 0.18$ GeV^2, $m_u = m_d = 0.23$ GeV/c^2, $m_s = 0.35$ GeV/c^2, $b = 1.83$ GeV^{-2}, $\alpha_{\{3\}} = 4$ GeV^{-2}. Fragmentation iterates until string masses are too low to allow further breaking.

• Fusion leads to a reduction of multiplicities, a slight increase of $\langle p_T^2 \rangle$, the cumulative effect is enhanced, and long range rapidity correlations decrease.

2.4 Rescattering of secondaries

• A very simple rescattering model with no space-time evolution is introduced to better reproduce strangeness/antibaryon enhancement at SPS (string junction migration has been introduced in other models, e.g. DPMJET and HIJING); it will allow to tune the initial state parameters.

• Threshold density is $dN/(dydp_T)|_{min} = 17$, rapidity and p_T range are 1.5 and 0.3 GeV/c respectively. All scattering probabilities are taken equal for all reactions (except for Ω production $(\times 2)$ and nucleon-antinucleon annihilation $(\times 10)$).

• Included: $\pi N \to \pi N$, $\pi\pi \to \pi\pi$, $\pi Y \to \pi Y$, $\pi\Xi \to \pi\Xi$, $KN \to KN$, $KY \to KY$, $\pi N \to KY$, $\pi\pi \to K\bar{K}$, $\pi Y \to K\Xi$, $\pi\Xi \to K\Omega$, $\bar{K}N \to \phi Y$ and $N\bar{N} \to \pi\pi$, $Y = \Sigma, \Lambda$. Decay of unstable particles follows JETSET (that of π^0's is forbidden).

• Consequences: Y, ϕ enhancement, $\bar{N}$ annihilation, slightly larger stopping.

2.5 Comparison to experimental data

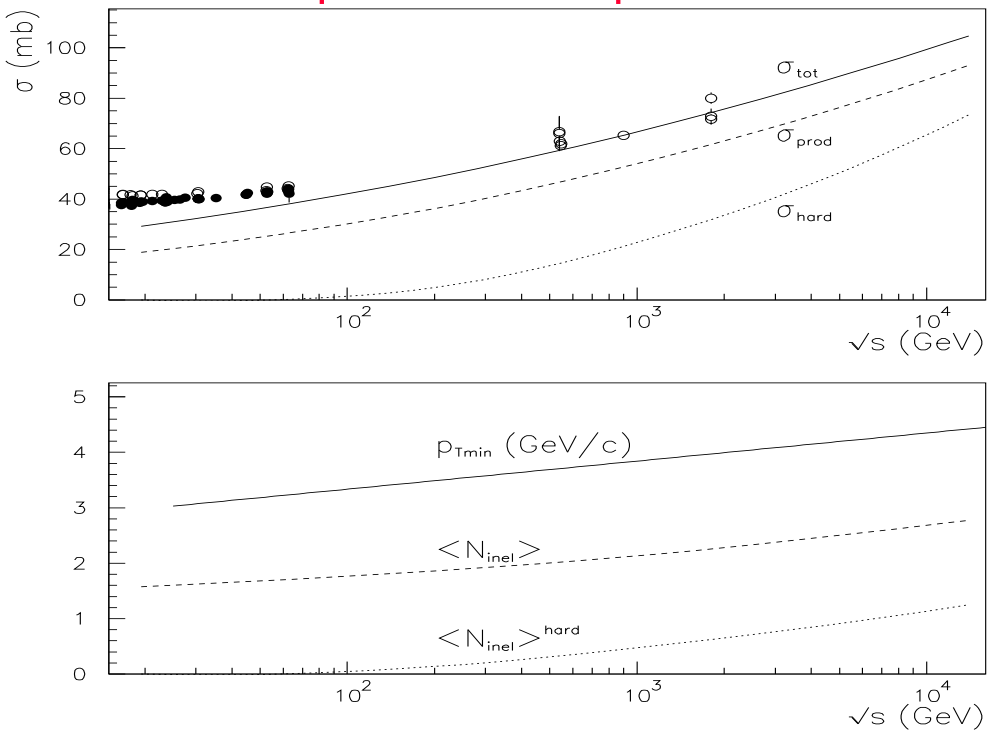

Figure 1: Upper plot: Comparison with experimental data for total cross sections in pp (filled circles) and $\bar{\mathrm{p}}$p (open circles) collisions. Lower plot: p_{Tmin}, and mean number of total and hard inelastic collisions per event, versus $\sqrt{s}$.

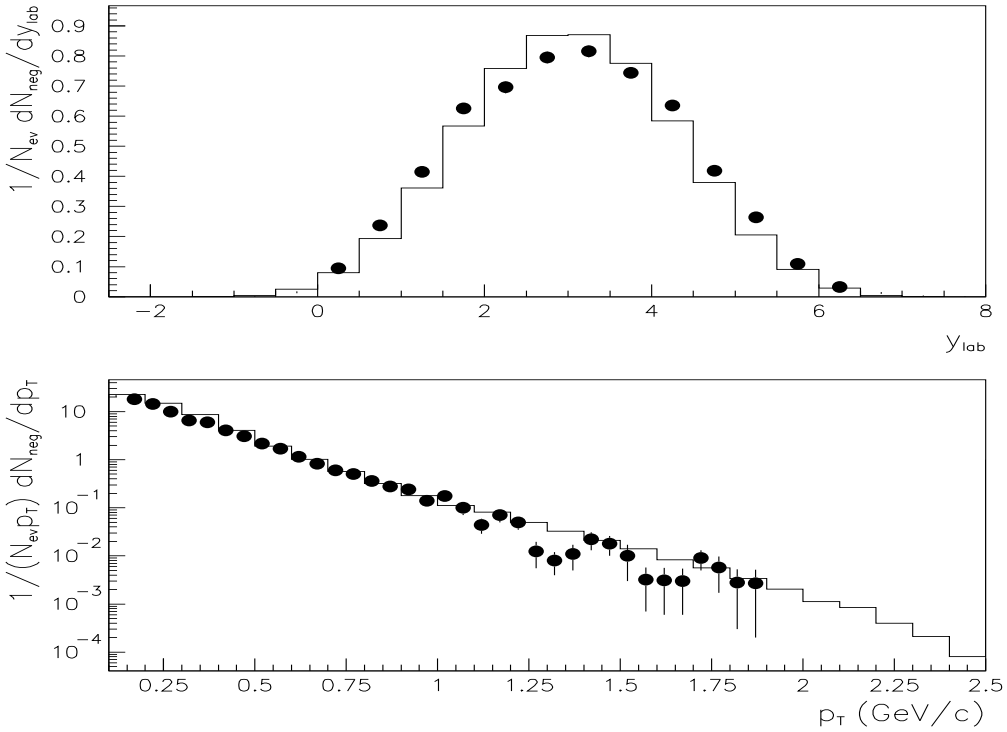

Figure 2: Results of the code for the rapidity distribution (upper plot), and the p_T distribution for particles with $2 < y_{lab} < 4$ (lower plot), of negative particles in minimum bias pp collisions at $p_{lab} = 200$ GeV/c, compared with experimental data.

	No fusion	Fusion	Experiment
charged	7.89	7.81	7.69 ± 0.06
negatives	2.95	2.90	2.85 ± 0.03
p	1.18	1.19	1.34 ± 0.15
π^+	3.40	3.33	3.22 ± 0.12
π^-	2.69	2.63	2.62 ± 0.06
π^0	3.73	3.68	3.34 ± 0.24
K^+	0.31	0.32	0.28 ± 0.06
K^-	0.18	0.18	0.18 ± 0.05
Λ	0.223	0.231	0.096 ± 0.010
$\bar{\Lambda}$	0.029	0.033	0.0136 ± 0.0040
$\bar{\mathrm{p}}$	0.059	0.070	0.05 ± 0.02

Table 1: Results in the model for mean multiplicities of different particles in minimum bias pp collisions at $p_{lab} = 200$ GeV/c, without and with string fusion, compared with experimental data.

	No fusion	Fusion	Experiment
p	1.20	1.21	1.20 ± 0.12
π^+	4.04	3.94	4.10 ± 0.26
π^-	3.32	3.23	3.34 ± 0.20
π^0	4.47	4.38	3.87 ± 0.28
K^+	0.38	0.38	0.33 ± 0.02
K^-	0.25	0.24	0.22 ± 0.01
Λ	0.245	0.251	0.13 ± 0.01
$\bar{\Lambda}$	0.045	0.049	0.020 ± 0.005
$\bar{\mathrm{p}}$	0.088	0.100	0.063 ± 0.002

Table 2: Results in the model for mean multiplicities of different particles in minimum bias pp collisions at $\sqrt{s} = 27.5$ GeV, without and with string fusion, compared with experimental data.

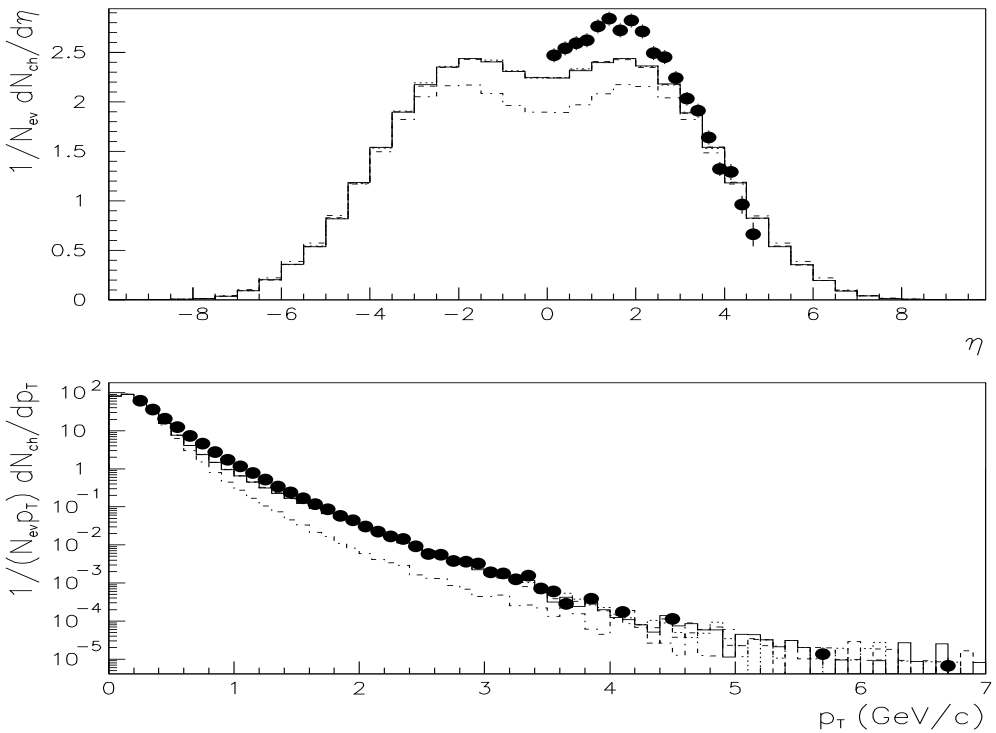

Figure 3: Results of the code for the pseudorapidity distribution (upper plot), and the p_T distribution for particles with $|\eta| < 2.5$ (lower plot), of charged particles in minimum bias $\bar{\mathrm{p}}\mathrm{p}$ collisions at $\sqrt{s} = 200$ GeV, compared with experimental data. Solid lines are the results with GRV 94 LO parton densities, dashed lines with CTEQ5L, dotted lines with GRV 98 HO and dashed-dotted lines results without semihard contribution.

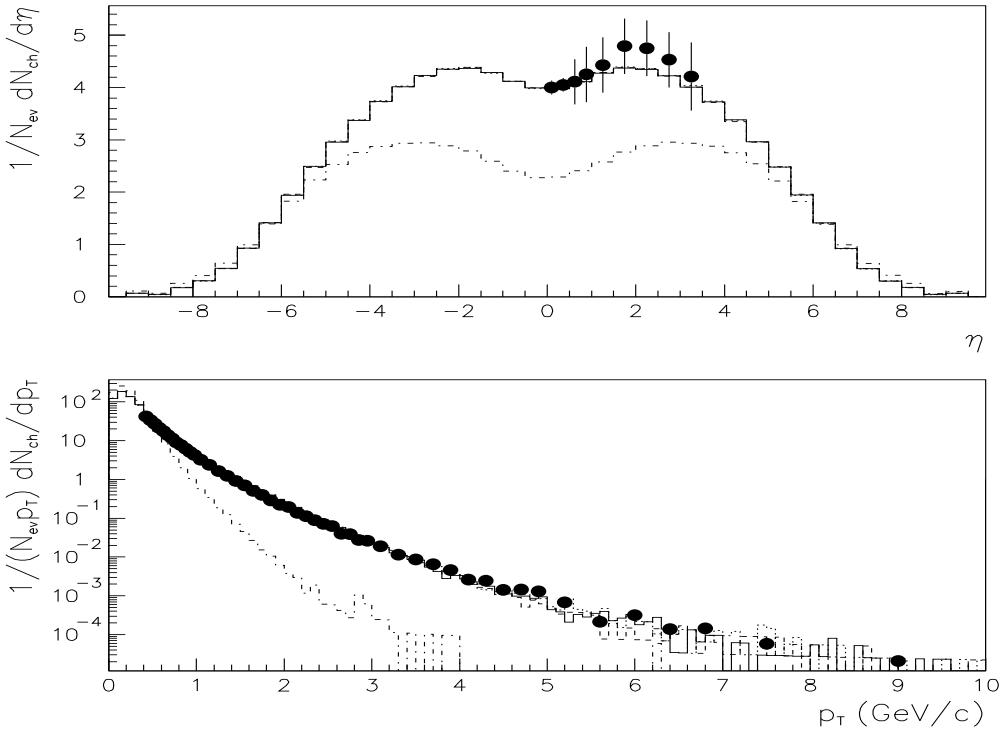

Figure 4: Results of the code for the pseudorapidity distribution (upper plot), and the p_T distribution for particles with $|\eta| < 1$ (lower plot), of charged particles in minimum bias $\bar{\mathrm{p}}\mathrm{p}$ collisions at $\sqrt{s} = 1.8$ TeV, compared with experimental data. Line convention is the same as in Fig. 3.

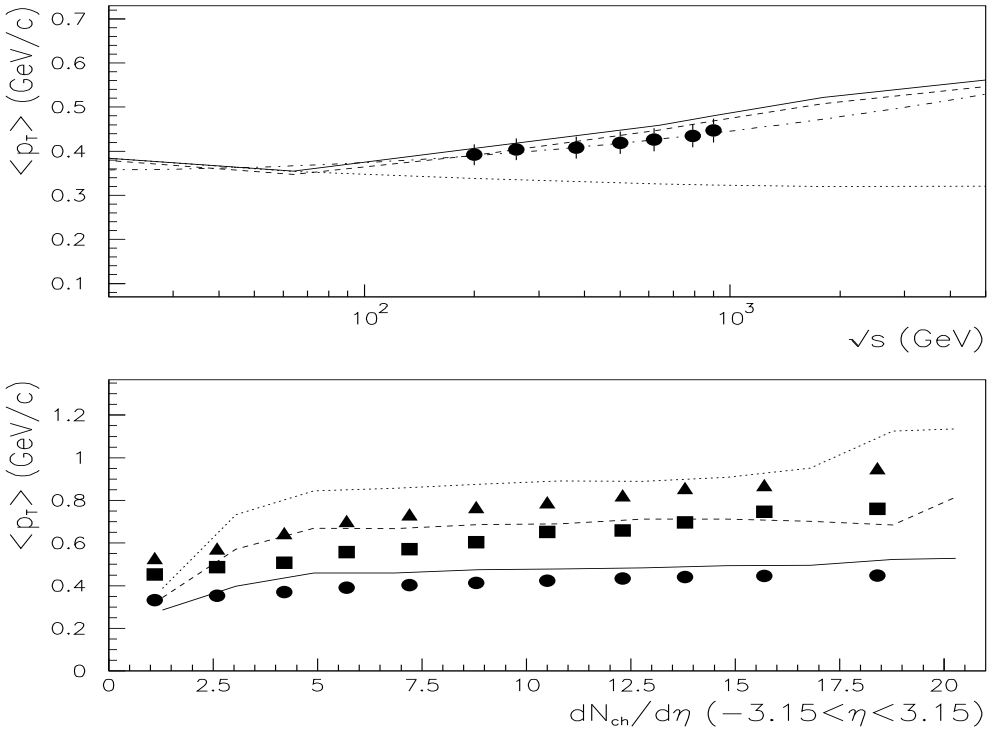

Figure 5: Upper plot: results of the code without hard part (dotted line), without string fusion (dashed line) and with string fusion (solid line) for $\langle p_T \rangle$ of charged particles with $|\eta| < 0.5$ in $\bar{\mathrm{p}}\mathrm{p}$ collisions, compared with UA1 data and a parametrization given in this reference (dashed-dotted line). Lower plot: results of the code for $\pi^{\pm}$ (solid line), $K^{\pm}$ (dashed line) and $\bar{\mathrm{p}}$ (dotted line) in $\bar{\mathrm{p}}\mathrm{p}$ collisions at $\sqrt{s} = 1.8$ TeV, compared with E735 data for $\pi^{\pm}$ (circles), $K^{\pm}$ (squares) and $\bar{\mathrm{p}}$ (triangles).

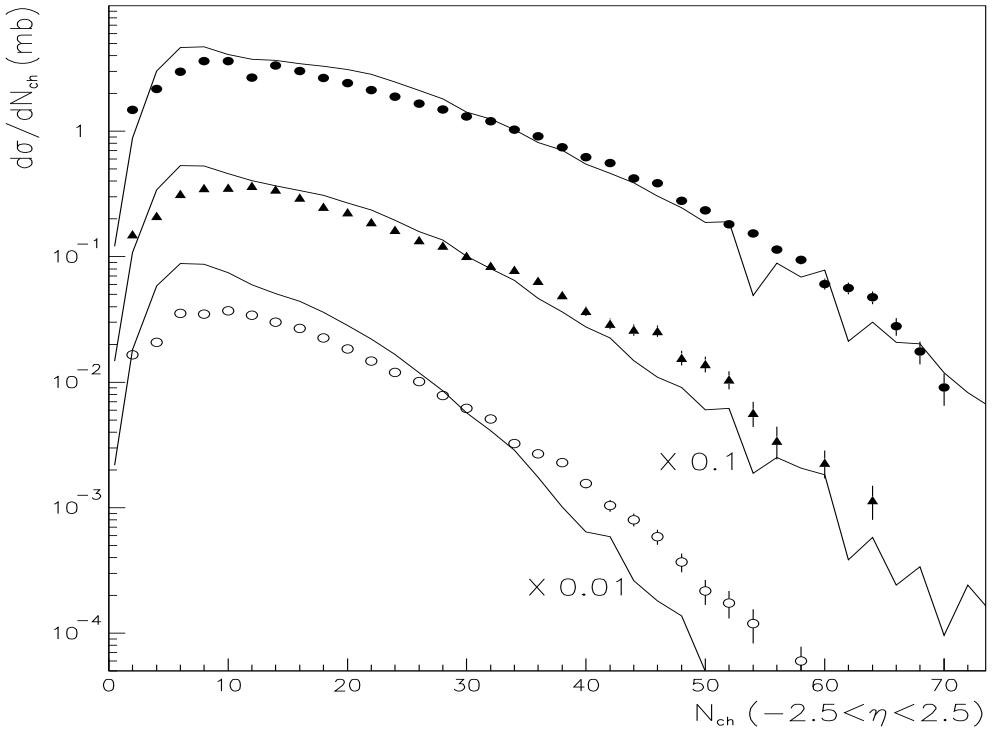

Figure 6: Results in the model (solid lines, arbitrarily normalized) for topological cross sections of charged particles with $|\eta| < 2.5$ in $\bar{\mathrm{p}}\mathrm{p}$ collisions, compared with experimental data. Upper curves and data correspond to $\sqrt{s} = 0.9$ TeV, those in the middle (multiplied by 0.1) to $\sqrt{s} = 0.5$ TeV, and lower curves and data (multiplied by 0.01) to $\sqrt{s} = 0.2$ TeV.

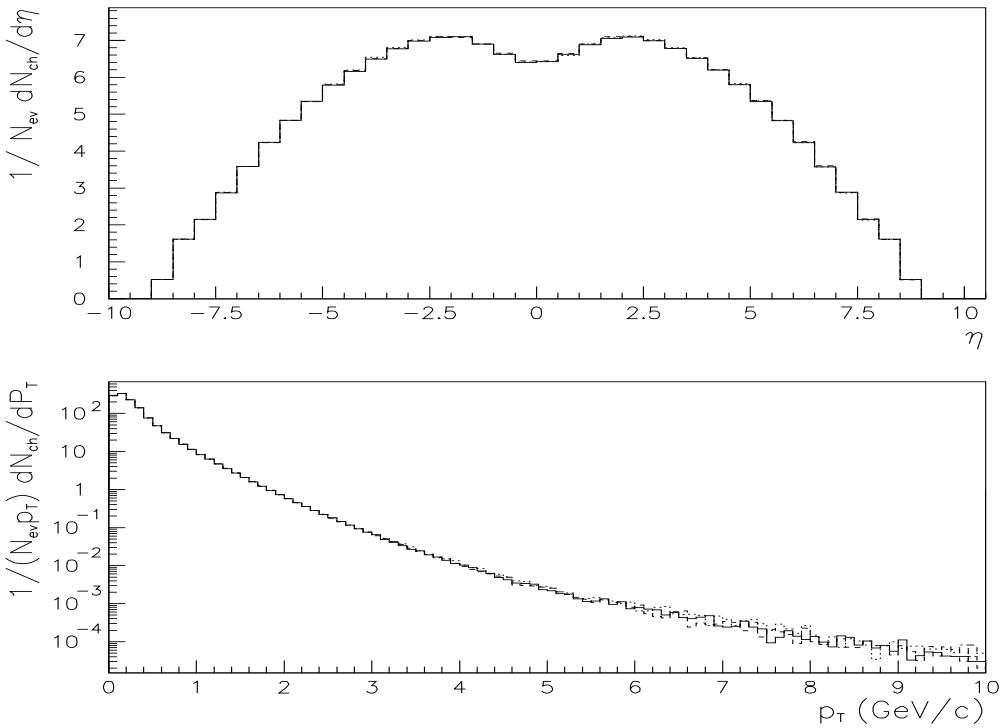

Figure 7: Results of the code for the pseudorapidity distribution (upper plot), and the p_T distribution for particles with $|\eta| < 2.5$ (lower plot), of charged particles in minimum bias pp collisions at $\sqrt{s} = 14000$ GeV. Line convention is the same as in Fig. 3 (the dashed-dotted line is absent).

	No fusion	Fusion	Experiment
pS	5.01	4.86	5.10 ± 0.20
pAr	5.31	5.12	5.39 ± 0.17
pAg	6.57	6.28	6.2 ± 0.2
pXe	6.89	6.56	6.84 ± 0.13
pAu	7.54	7.16	7.0 ± 0.4

Table 3: Results in the model for mean multiplicities of negative particles in minimum bias pA collisions at $p_{lab} = 200$ GeV/c, without and with string fusion, compared with experimental data for pS, pAr, pAg, pXe and pAu.

	NF	F	FR	Experiment
negatives	108.2	101.3	100.7	98 ± 3
K^+	9.7	10.4	10.8	12.5 ± 0.4
K^-	7.1	7.2	7.4	6.9 ± 0.4
Λ	5.0	5.9	6.0	9.4 ± 1.0
$\bar{\Lambda}$	0.4	1.1	1.2	2.2 ± 0.4
$\bar{\mathrm{p}}$	0.82	3.23	2.80	
Ξ^-	0.024	0.186	0.205	
$\bar{\Xi}^+$	0.028	0.097	0.102	
Ω^-	0.001	0.007	0.010	
$\bar{\Omega}^+$	0.001	0.005	0.007	

Table 4: Results in the model for mean multiplicities of different particles in central ($b \leq 1.3$ fm) SS collisions at $\sqrt{s} = 19.4$ GeV per nucleon, compared with experimental data. Results are presented without fusion (NF), with fusion (F), and with fusion and rescattering (FR).

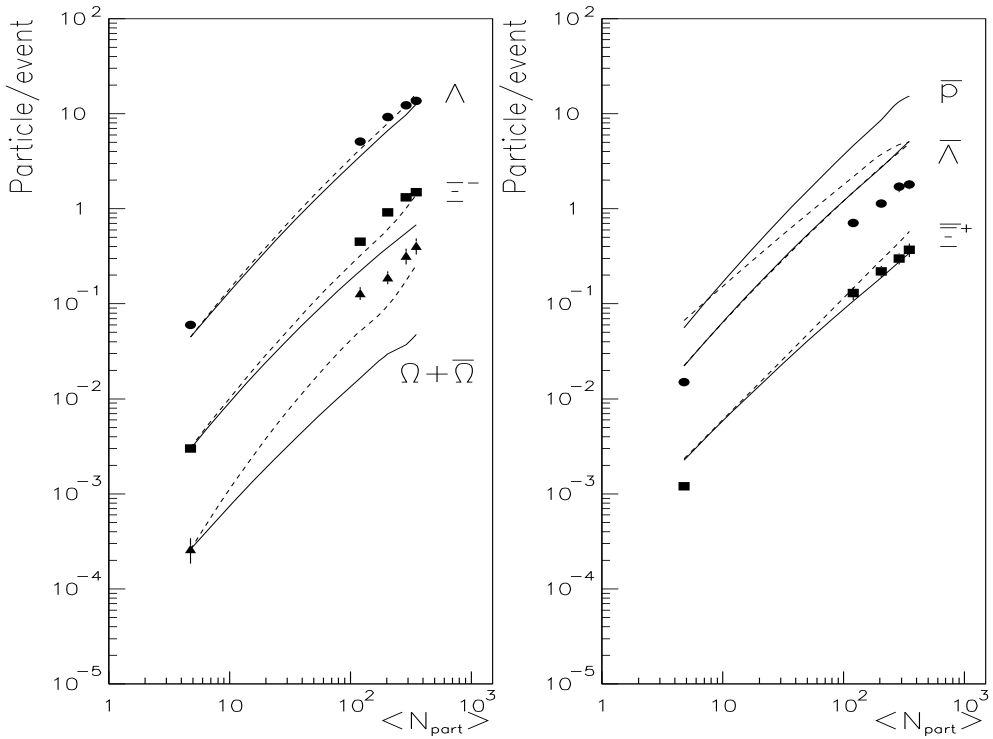

Figure 8: Yields per unity of rapidity at central rapidity, as a function of the number of wounded nucleons, for Λ, Ξ^- and $\Omega^- + \bar{\Omega}^+$ (left), and for $\bar{p}$, $\bar{\Lambda}$ and $\bar{\Xi}^+$ (right), for pPb collisions and four different centralities in PbPb collisions at SPS energies. Full lines represent our calculation with string fusion, and dashed lines with fusion and rescattering. Experimental data are from the WA97 Collaboration.

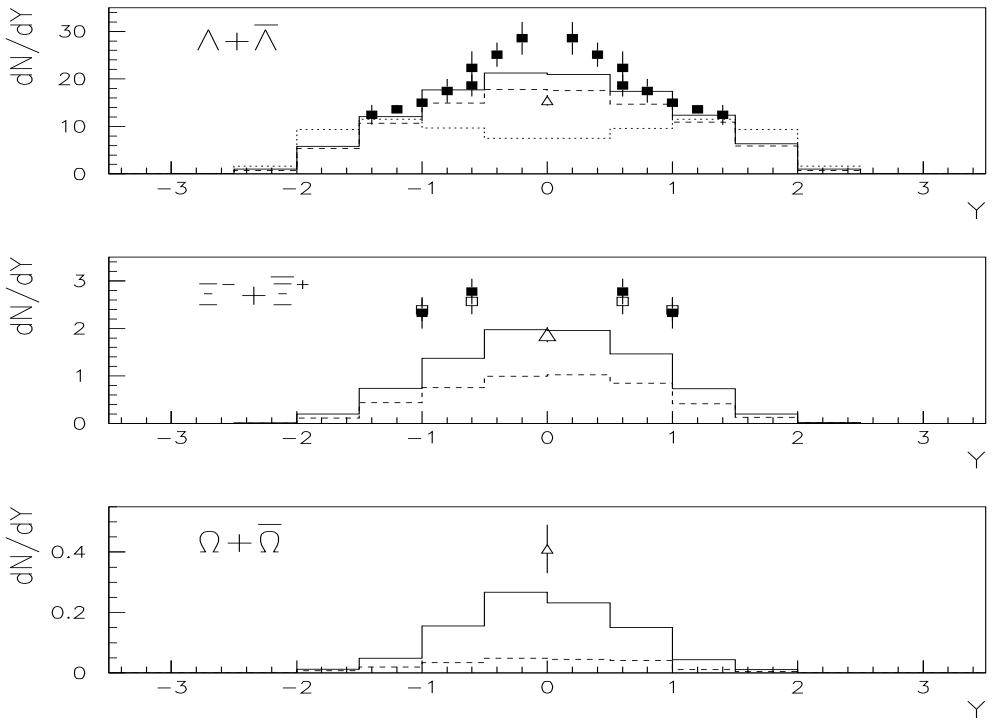

Figure 9: Results in the model (dotted line: without fusion, dashed line: with fusion, solid line: with fusion and rescattering) for strange baryon production in central PbPb collisions (5 % centrality) at SPS compared with experimental data from the WA97 Collaboration (triangles) and the NA49 Collaboration (squares).

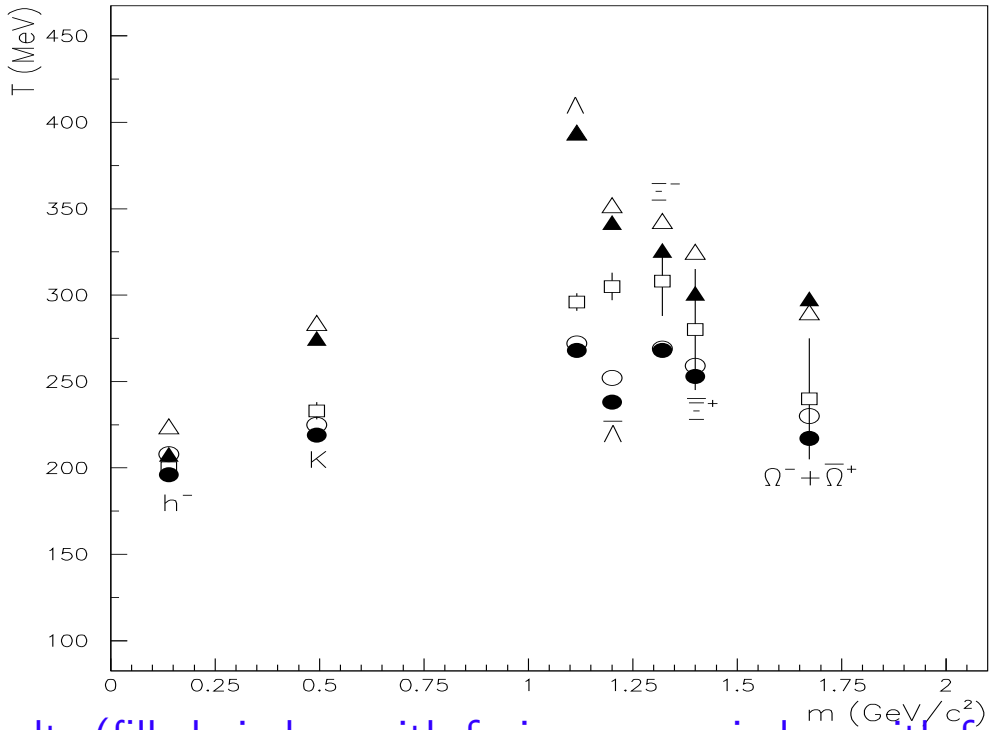

Figure 10: Results (filled circles: with fusion, open circles: with fusion and rescattering) for the inverse exponential slope of the m_T distributions at midrapidity of different particles versus the mass of the particles in central (5 % centrality) PbPb collisions at SPS, compared with the experimental data of the WA97 Collaboration (3.5 % centrality, open squares). We also present predictions for the same collisions at RHIC with fusion, filled triangles, and with fusion and rescattering, open triangles.

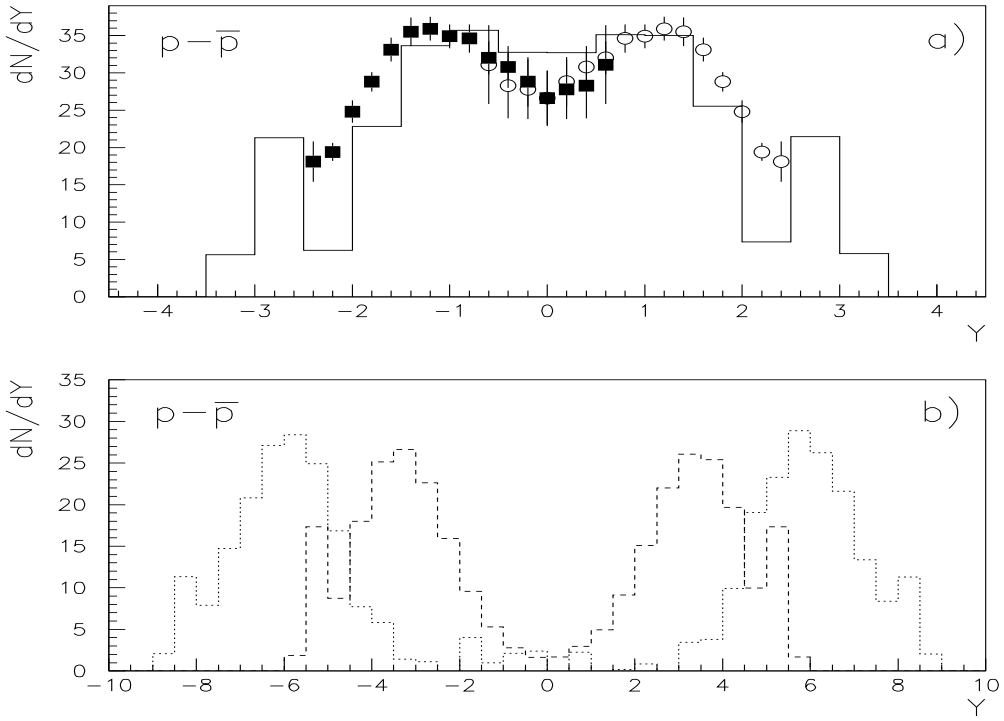

Figure 11: Results in the model for the $p - \bar{p}$ rapidity distribution in central (5 % centrality) PbPb collisions at SPS (a), solid line, and RHIC and LHC (b), dashed and dotted lines respectively, compared with experimental data at SPS.

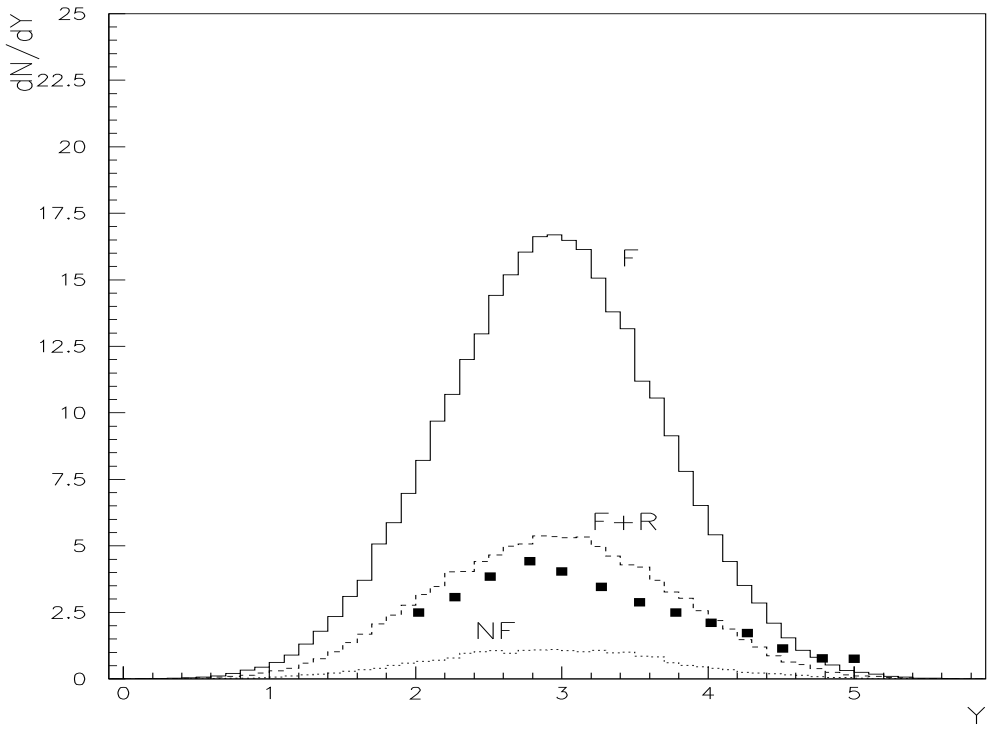

Figure 12: Results in the model (dotted line: without fusion, solid line: with fusion, dashed line: with fusion and rescattering) for the $\bar{p}$ rapidity distribution in central (5 % centrality) PbPb collisions at SPS, compared with experimental data.

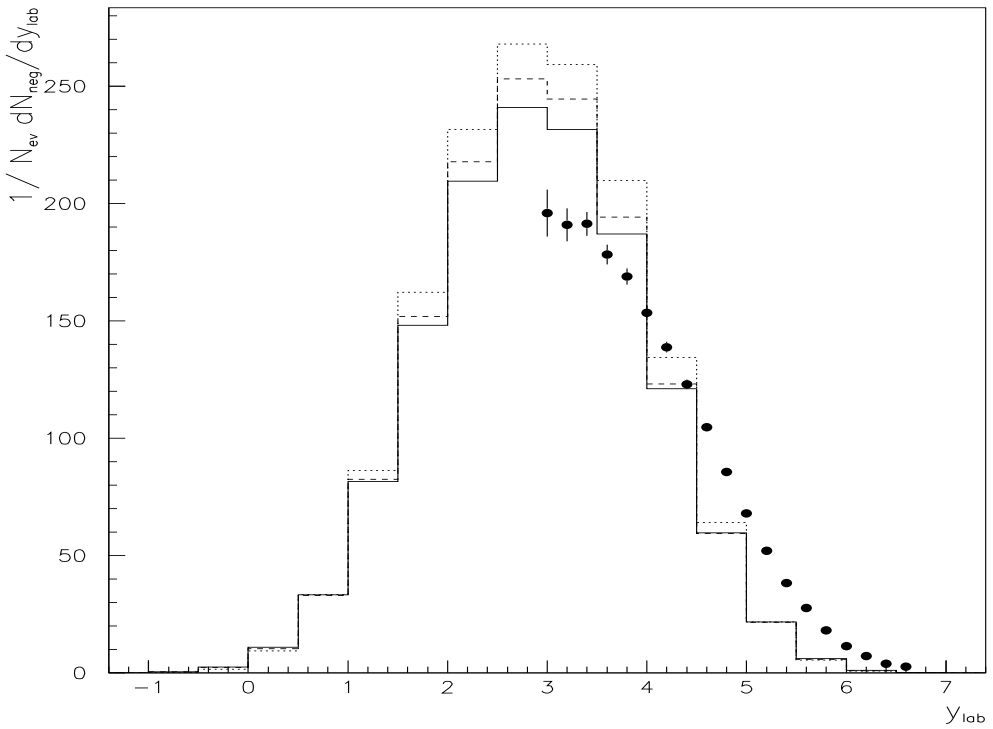

Figure 13: Results in the model for the rapidity distribution of negative particles in central (5 % centrality) PbPb collisions at $\sqrt{s} = 17.3$ GeV per nucleon, without fusion (dotted line), with fusion (dashed line) and with fusion and rescattering (solid line), compared with data from NA49.

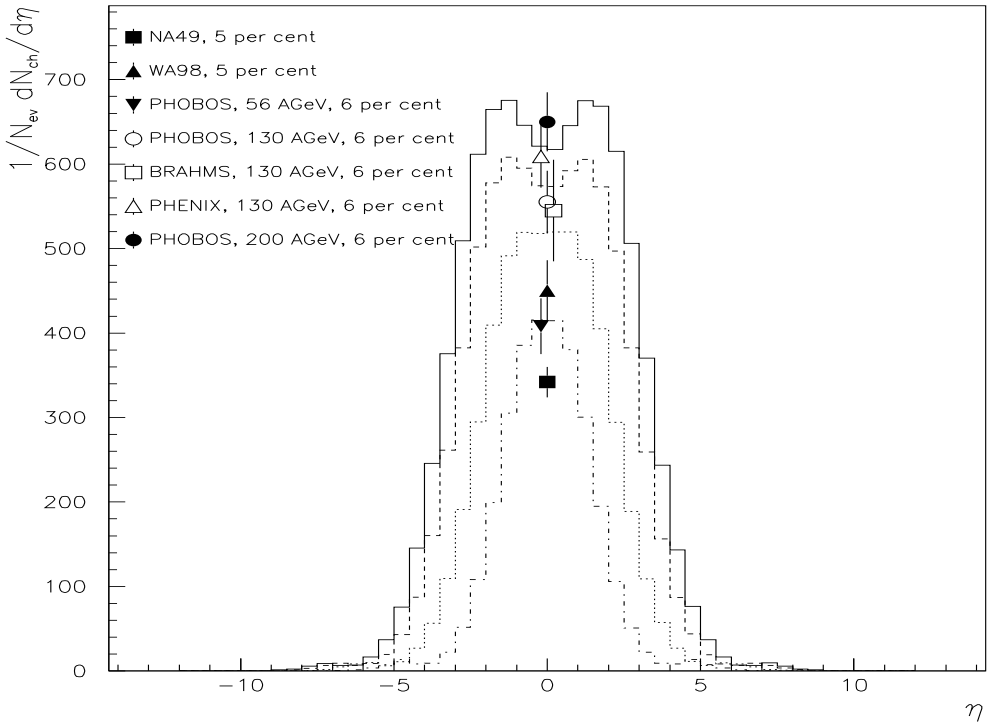

Figure 14: Results of the model for the pseudorapidity distribution of charged particles for central (5 %) PbPb collisions at 17.3 GeV per nucleon in the center of mass (dashed-dotted line), and central (6 %) AuAu collisions at 56 (dotted line), 130 (dashed line) and 200 (solid line) GeV per nucleon in the center of mass, compared with experimental data at SPS and RHIC.

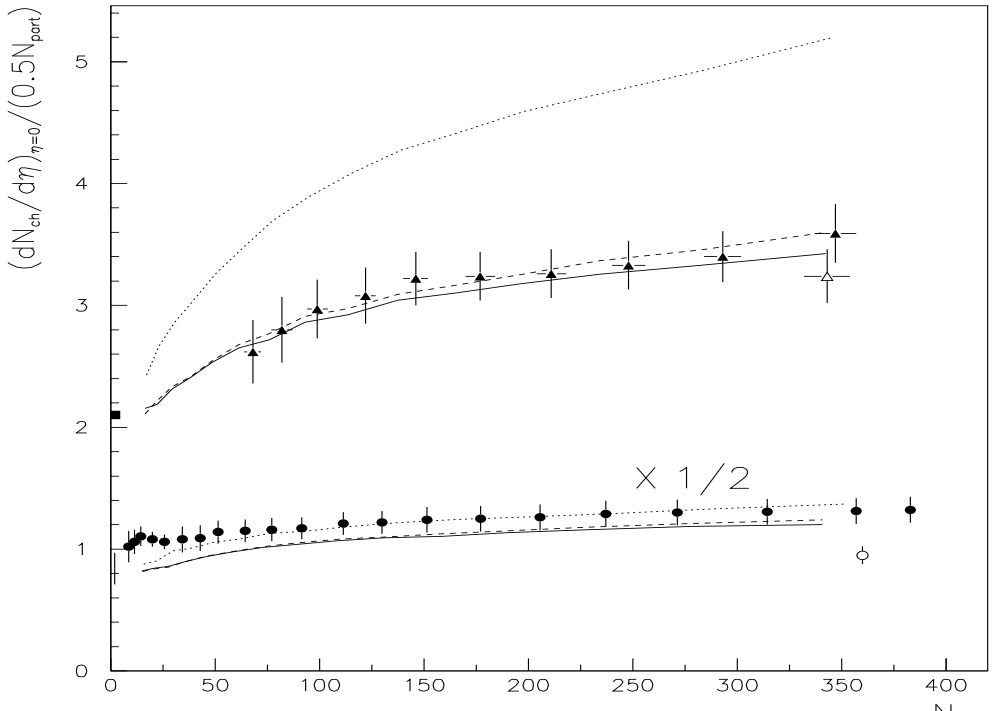

Figure 15: Comparison with experimental data in PbPb collisions at 17.3 GeV/n (multiplied by 1/2, lower curves and symbols) and in AuAu collisions at 130 GeV/n (upper curves and symbols); also the experimental number for $\bar{\mathrm{p}}\mathrm{p}$ collisions at 130 GeV/n is given, filled square. Experimental data are from PHENIX (filled triangles), PHOBOS (open triangle), WA98 (filled circles) and NA49 (open circle). Curves are results of the model without fusion or rescattering (dotted lines), with fusion (dashed lines) and with fusion and rescattering (solid lines).

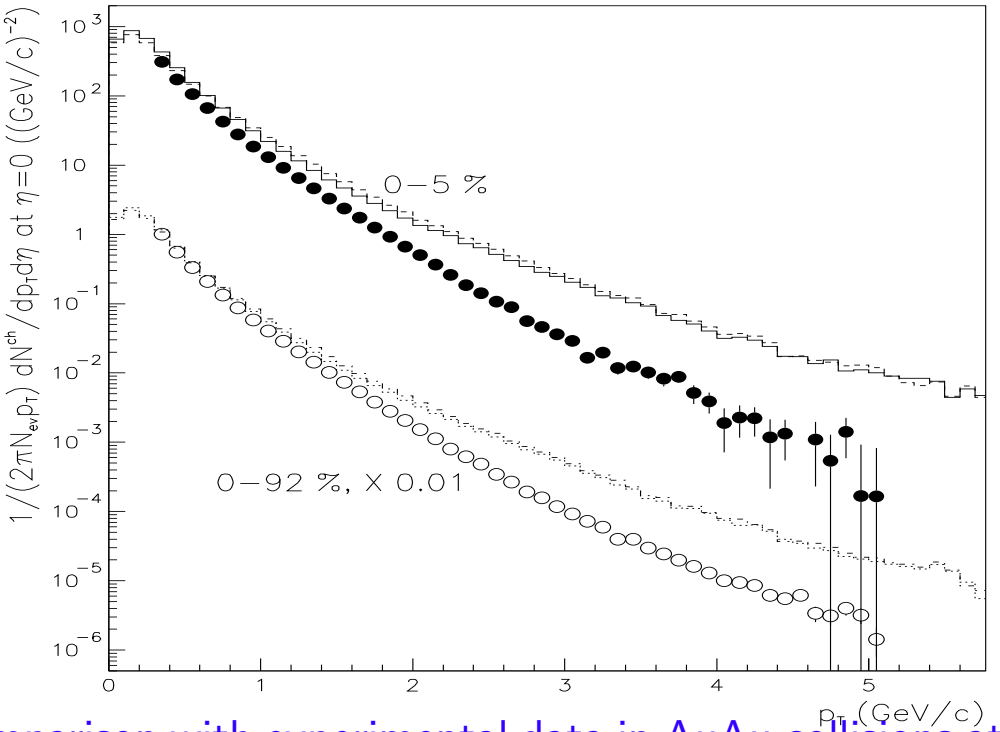

Figure 16: Comparison with experimental data in AuAu collisions at 130 GeV per nucleon in the center of mass, for central collisions (solid and dashed lines and filled circles) and for minimum bias collisions (multiplied by 0.01, dotted and dashed-dotted lines and open circles). Data are from PHENIX; solid and dotted lines are results of the model with string fusion, dashed and dashed-dotted lines with string fusion and rescattering.

Ratio	NF	F	FR	BRAHMS	PHENIX	PHOBOS	STAR
$\bar{\mathrm{p}}/\mathrm{p}$ $(\eta \sim 0)$	0.81	0.85	0.80	0.64±0.04 ±0.06 $(y \sim 0)$	0.64±0.01 ±0.07	0.60±0.04 ±0.06	0.65±0.01 ±0.07
$\bar{\mathrm{p}}/\mathrm{p}$ $(y \sim 2)$	0.38	0.50	0.38	0.41±0.04 ±0.06			
$\bar{\Lambda}/\Lambda$ $(\eta \sim 0)$	0.85	0.87	0.87		0.75±0.09		0.74±0.04
K^-/K^+ $(\eta \sim 0)$	0.92	0.97	0.96			0.91±0.07 ±0.06	
π^-/π^+ $(\eta \sim 0)$	1.02	1.02	1.01			1.00±0.01 ±0.02	

Table 5: Different particle ratios in central (10 %) AuAu collisions at 130 GeV per nucleon in the center of mass, in the model without string fusion or rescattering (NF), with string fusion (F) and with string fusion and rescattering (FR), for particles with $p_T > 0.2$ GeV/c, compared with experimental data.

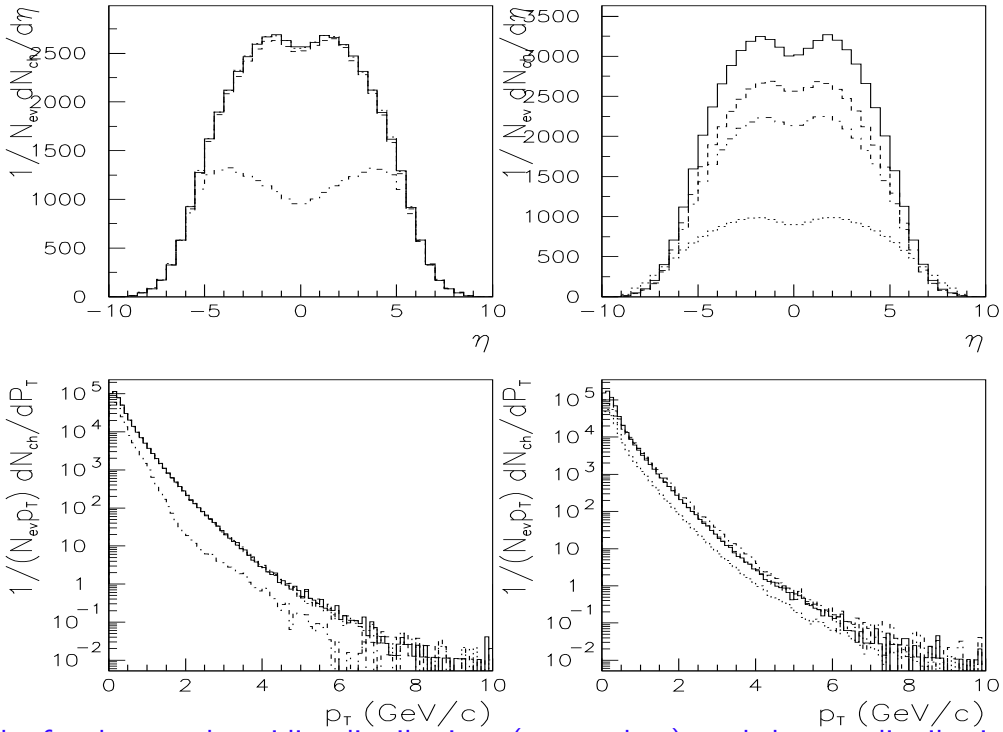

Figure 17: Results for the pseudorapidity distributions (upper plots), and the p_T distributions for particles with $|\eta| < 2.5$ (lower plots), of charged particles in central ($b \leq 3.2$ fm) PbPb collisions at $\sqrt{s} = 5500$ GeV per nucleon. Left: solid lines — EKS98 parametrization of parton densities inside nuclei, dashed lines — parametrization as F_{2A}, dotted lines — without modification, and dashed-dotted lines — without semihard contribution. Right: solid lines — without string fusion, dashed lines — with string fusion, dotted lines — nucleon-nucleon results scaled by the number of wounded nucleons (382.1/2), and dashed-dotted lines — results with string fusion and rescattering.

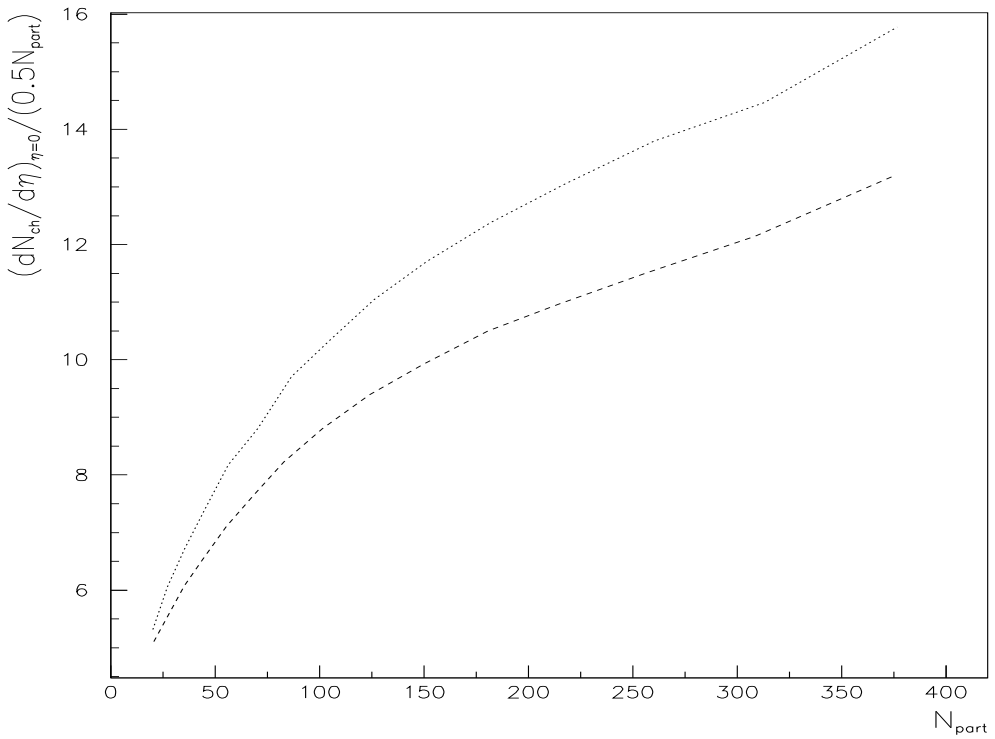

Figure 18: The same as in Fig. 15, but for PbPb collisions at 5.5 TeV per nucleon in the center of mass.

3. Instructions for installation and use

• The code psm-1.0, in Fortran 77, can be downloaded in http://fpaxp1.usc.es/phenom/, http://www.uco.es/~fa1arpen/ or by anonymous ftp at ftp.uco.es, folder pub/fa1arpen; size ~ 900 Kb.

• Contact persons: D.Sousa (sousa@ect.it) and NA (Nestor.Armesto@cern.ch).

• After uudecode, gunzip and tar xvf, you will find a manual, manpsm-1.0.ps.

• To compile, just do
g77 *-1.0.f (link with CERNLIB)
If PDFLIB 8.04 is not available, see the manual.

• To run: options in file psminput:

PB *BEAM: N,P,PBAR,D,HE,BE,B,C,O,AL,SI,S,AR,CA,CU,AG,XE,W,AU,PB,U*

PB *TARGET: N,P,PBAR,D,HE,BE,B,C,O,AL,SI,S,AR,CA,CU,AG,XE,W,AU,PB,U*

5500. *Ecm/NUCLEON: 10. < Ecm/NUCLEON (GeV) < 15000.*

FIXB *IMPACT PARAMETER: FIXB or RANB*

3.0 *B: 0 ≤ b ≤ B (fm), in case of IMPACT=FIXB*

10 *NEVENT: 1,...*

T *HARD PART: T (D: ONLY ACTIVE FOR Ecm/NUCLEON ≥ 25. GeV) or F*

T *STRING FUSION: T (D) or F*

T *RESONANCE DECAY: T (D) or F*

T *RESCATTERING: T (D) or F (WARNING!!!!: EXTREMELY TIME CONSUMING, BETTER NOT TO BE USED FOR Ecm/NUCLEON > 200 GeV WITHOUT CARE)*

1505 *NUCLEON PDF SET: PDFLIB NUMBERING SCHEME AS NPTYPE*1000+NGROUP*100+NSET (D: 1505, GRV 94 LO), if HARD PART=T*

1 *NUCLEAR SF CORRECTIONS: 0=NO CORRECTION, 1=EKS98 CORRECTIONS (D), 2=ESKOLA-QIU-CZYZEWSKI CORRECTION AS F2, if HARD PART=T*

• To define centralities, run a reasonable number of minimum bias events (RANB) and use impar-psm.f on file impar-psm.dat (there you will find b, n^A_{woun}, n^B_{woun} and n_{coll} for each generated event).

• Control file: psm.log.

• Output: in the form of HBOOK histograms in hist-1.0.f or hisalice.f, to be modified by the user.

• Final particles: stored in common blocks LUJETS (before rescattering) and RUJETS (after rescattering; identical to LUJETS if rescattering has been switched off). Particle numbering scheme is the standard of PYTHIA.

• CPU-times: hard contribution, fusion and, above all, rescattering increase them; use rescattering with care.

• Example: 10 PbPb collisions at 5.5 TeV/nucleon, b < 3 fm, took yesterday in lxplus (PC cluster at CERN) ~ 280 minutes with rescattering.

• Tested in Sun, DEC alpha and PC under linux.

• Key parameters: in common blocks at the end of file psm-1.0.f, and in subroutine PSLUNSE for PYTHIA/ARIADNE/JETSET options (please manipulate with care).

• FUTURE: phase transition, inclusion of hard part in the interacting part, heavy flavor production.